Research Square

Preprints are preliminary reports that have not undergone peer review.
They should not be considered conclusive, used to inform clinical practice,
or referenced by the media as validated information.

APH-1A and CDK5 Expression Correlates with Tau Hyperphosphorylation and Its Attenuation by Brahmi and Donep-M in STZ induced Alzheimer's Disease Model

Umesh Prasad Sah Hathi
Jawaharlal Nehru University
Abhishek Kumar
Jawaharlal Nehru University
Jyotsna Arora
Jawaharlal Nehru University
Suneel Kateriya
skateriya@jnu.ac.in

Jawaharlal Nehru University

Research Article

Keywords: Alzheimer's disease, Neural cilia, Tau phosphorylation, AFM, Confocal microscopy

Posted Date: October 31st, 2026

DOI: https://doi.org/10.21203/rs.3.rs-11257702/v1

License: This work is licensed under a Creative Commons Attribution 4.0 International License.
Read Full License

Additional Declarations: No competing interests reported.

APH-1A and CDK5 Expression Correlates with Tau Hyperphosphorylation and Its Attenuation by Brahmi and Donep-M in STZ induced Alzheimer's Disease Model.

Umesh Prasad Sah Hathi[1], Abhishek Kumar[1], Jyotsna Arora[1, 2], Suneel Kateriya[1, $]

[1]Laboratory of Optobiotechnology, School of Biotechnology, Jawaharlal Nehru University, New Delhi-110067, India.

[2]Centre for Ayurveda Biology, School of Sanskrit and Indic Studies, Jawaharlal Nehru University, New Delhi-110067, India.

[$]Correspondance: Suneel Kateriya (skateriya@jnu.ac.in)

Abstract

Alzheimer's disease (AD) is a progressively characterized neurodegenerative condition marked by molecular instability, neuronal dysfunction and abnormal tau buildup. Identification of disease-associated molecular signatures that can be experimentally validated in neuronal models may provide biologically relevant biomarkers and targets for therapeutic intervention. Here, we employed an integrated transcriptomic and cellular approach to identify and validate biomarkers associated with AD pathology. Differential transcriptomic analysis of (AD versus control) samples was used to prioritize candidate genes, followed by experimental validation in a streptozotocin (STZ) induced SH-SY5Y cells. Among the selected genes, anterior pharynx defective 1A (APH-1A) and cyclin dependent kinase (CDK5) were experimentally validated and further correlated to tau pathology by quantifying phosphorylation of tau at serine 396 (p-Tau Ser396) using confocal fluorescence microscopy. Complementary atomic force microscopy (AFM) was employed to characterize STZ-associated cellular morphological alterations. STZ exposure induced an AD-like neuronal phenotype characterized by associated cellular structural abnormalities. Importantly, co-treatment with *Bacopa monnieri* (Brahmi) attenuated STZ-associated tau Ser396 phosphorylation and improved the cellular phenotype. The effects of Brahmi were further compared with those of established anti-Alzheimer's drugs, Donep-M (Donepezil and Memantine) together, which similarly reduced p-Tau Ser396-associated alterations. The concordance between molecular biomarker validation and imaging-based phenotypic responses warrants further investigation of underlying molecular mechanisms. Collectively, our findings establish a transcriptome-to-cellular validation framework in which APH-1A and CDK5 represent experimentally supported AD-associated biomarkers. This integrated strategy provides a foundation for connecting human AD molecular signatures with measurable neuronal phenotypes and evaluating potential therapeutic interventions.

Keywords: Alzheimer's disease, Neural cilia, Tau phosphorylation, AFM, Confocal microscopy.

Introduction

AD is a progressive neurodegenerative disorder characterized by the accumulation of pathological amyloid beta (Aβ) and tau, synaptic dysfunction, neuronal degeneration, and progressive impairment of cognitive function(Grundke-Iqbal et al. 1986; Braak and Braak 1991; Alonso et al. 1997; Thal et al. 2002; Tiraboschi et al. 2004; Vossel et al. 2010; Furcila, DeFelipe, and Alonso-Nanclares 2018; Busche and Hyman 2020). Although amyloid and tau pathology represent major neuropathological hallmarks, the mechanistic understanding connecting early cellular dysfunction to neuronal structural and functional deterioration remain incompletely resolved. Recent human studies have demonstrated that soluble and site-specific phospho-tau species can provide sensitive indicators of AD-associated pathology, with particular phosphorylation sites reflecting early stages of tau dysregulation and disease progression(Cavallini et al. 2013; Barthélemy et al. 2023; Hernández-Hernández et al. 2025; Islam et al. 2025). Therefore, identification of molecular alterations that converge on tau pathology may provide biologically relevant biomarkers and potential therapeutic targets for AD.

High-throughput transcriptomic approaches provide an opportunity to identify disease-associated molecular signatures directly from human AD tissue and to prioritize candidate genes for experimental validation(Wan et al. 2020; Eteleeb et al. 2024; Stephens et al. 2025). However, transcriptomic signatures generated from postmortem brain or other human diseased AD-datasets do not necessarily represent functionally relevant neuronal phenotypes(Hou et al. 2025). Experimental validation in neuronal cellular models is therefore essential to distinguish robust disease-associated candidates from transcriptional changes that may reflect tissue heterogeneity, disease stage, or secondary responses(Shin et al. 2026). In the present study, we adopted a transcriptome-guided strategy to identify AD-associated molecular candidates and subsequently evaluated their expression in an experimentally induced neuronal AD-like model. From an initial panel of eleven candidate genes identified through AD versus control transcriptomic analysis, APH-1A and CDK5 emerged as experimentally validated candidates following exposure of SH-SY5Y neuronal cells to STZ followed by treatment with Brahmi and anti-AD drugs (Donep-M).

APH-1A is an integral component of the γ-secretase complex and is directly relevant to amyloidogenic processing(Ma et al. 2005; Pardossi-Piquard et al. 2009). Experimental work has demonstrated that G protein-coupled receptor (GPCR) kinases (GRKs) phosphorylates APH-1A altering γ-secretase-associated conformational states and consequently regulate Aβ generation, providing a mechanistic link between APH-1A regulation and the amyloidogenic pathway(Todd et al. 2022). Thus, altered APH-1A expression in AD may reflect dysregulation of γ-secretase-dependent processing rather than representing merely a passive transcriptional signature. In parallel, CDK5 is a neuron-enriched serine/threonine kinase involved in neuronal cytoskeletal organization, synaptic function, and tau phosphorylation (B.-S. Li et al. 2000; Tanaka et al. 2001; Kesavapany et al. 2004; N. Miller et al. 2015). Recent kinase studies have demonstrated that CDK5/p25 can promote phosphorylation of tau at several AD-relevant sites, including Ser396(Cavallini et al. 2013). More recently, experimental studies have provided further evidence connecting pathological CDK5 activation with tau phosphorylation, neuronal structural damage, and synaptic dysfunction in AD models(Fu et al. 2025; Huang et al. 2017). Nevertheless, human postmortem data also indicate that the relationship between CDK5 activation and tau pathology is more complex than a simple linear kinase-tau relationship, emphasizing

the importance of experimentally validating CDK5-associated signatures in defined cellular models(Hernández-Hernández et al. 2025).

To experimentally model AD-associated neuronal stress, STZ treated SH-SY5Y cells have been increasingly used as an in-vitro model of AD-like cellular dysfunction. STZ exposure has been reported to induce cellular stress, altered insulin-related signaling, and tau-associated pathology in neuronal cells(Plaschke and Kopitz 2015; Kamat 2015; Kadhim et al. 2022; Biswas et al. 2016; Bagaméry et al. 2020, 2021; Sahu, Ahmad, and Mondal 2026). In particular, STZ treatment of SH-SY5Y cells has been shown to alter GSK3 signaling and increase tau-associated pathological responses, providing a cellular framework for investigating mechanisms associated with tau dysregulation(Bagaméry et al. 2020; Shandilya, Kesari, and Ruokolainen 2021; Bagaméry et al. 2021; Paszternák et al. 2025). Importantly, STZ induced neuronal pathology is not restricted to cell viability changes, but encompasses multiple molecular stress pathways that are relevant to AD-associated neurodegeneration(Singh, Tiwari, and Singh 2024; Shandilya, Kesari, and Ruokolainen 2021; Paszternák et al. 2025). This makes the model suitable for testing whether transcriptome-derived AD candidates are responsive to experimentally induced neuronal pathology.

Among the pathological consequences of AD-associated cellular stress, tau hyperphosphorylation represents a particularly relevant functional endpoint (B. Li et al. 2007; Cowan et al. 2010). Tau is a microtubule-associated protein whose pathological phosphorylation reduces its normal interaction with microtubules and promotes conformational changes and aggregation(Yu et al. 2009; Barthélemy et al. 2020). Ser396 is among the AD-associated phosphorylation sites of tau and has long been used experimentally to assess pathological tau phosphorylation(T. Li and Paudel 2006; Bramblett et al. 1993). Recent studies further emphasize that specific phospho-tau species can provide information about distinct stages of tau pathology and disease progression(Neddens et al. 2018; Regalado-Reyes et al. 2019; Chongtham et al. 2025). Thus, assessing phospho-tau Ser396 (p-Tau_Ser396) provides a molecular endpoint through which transcriptome-derived candidates can be connected to a disease-relevant neuronal phenotype.

Majorly, AD-associated tau pathology also has structural and biophysical consequences at the cellular level leading to the transformation in the neuronal cytoskeleton, membrane organization, and cell substrate interactions which can alter cellular morphology as well as mechanical properties(Hernández-Hernández et al. 2025; Barthélemy et al. 2020; Yu et al. 2009). AFM provides a complementary approach to conventional fluorescence imaging by enabling quantitative characterization of cellular topography(Legleiter and Kowalewski, n.d.; do Nascimento Amorim et al. 2024). Previous study in SH-SY5Y cells has demonstrated that AD-associated Aβ exposure can modify cytoskeletal organization and cellular mechanical properties, while AFM studies have established the feasibility of quantifying the elastic properties of differentiated and undifferentiated SH-SY5Y cells(Gao et al. 2018; Kruger et al. 2019; Kumari et al. 2020; Chen et al. 2023; Dague et al. 2022). Therefore, combining AFM with confocal microscopy provides an opportunity to link molecular tau pathology with cellular structural alterations, rather than relying solely on changes in fluorescence intensity.

Natural products with neuroprotective properties may provide complementary strategies for targeting multiple pathological pathways in AD(Mehla et al. 2020; Shalini, Neelakanta, and Sriranjini 2021; Basheer et al. 2022). *Bacopa monnieri* (Brahmi) is particularly interesting because experimental studies have reported effects on oxidative stress,

tau phosphorylation, tau aggregation, and AD-associated signaling(Vinod et al. 2022; Shalini, Neelakanta, and Sriranjini 2021; Dubey and Chinnathambi 2019; Basheer et al. 2022). A 2023 cellular study demonstrated that Brahmi extract reduced tau aggregation and phospho-tau-associated toxicity, while also modulating glycogen synthase kinase-3beta (GSK3β) and oxidative stress related pathways(Dubey et al. 2023). More recently, experimental work in an Aβ-induced AD model showed that Brahmi supplementation reduced phospho-tau and total tau abnormalities while modulating mitochondrial dysfunction and GSK3β/Wnt/β-catenin signaling(Sushma et al. 2024). These findings provide a biological rationale for evaluating Brahmi in an experimentally induced neuronal tauopathy model. However, whether Brahmi can reverse tau pathology associated with a transcriptome validated molecular signature, particularly APH-1A and CDK5, remains insufficiently characterized.

Clinically used anti-AD agents provide an essential pharmacological benchmark for evaluating such experimental interventions. Memantine and cholinesterase inhibitors such as donepezil are established symptomatic therapies, but their effects on molecular and structural phenotypes in experimentally induced neuronal AD-like models require further characterization(Biswas et al. 2016; Guler et al. 2024). Comparing Brahmi with established anti-AD pharmacological agents may therefore help determine whether its effects on pathological tau represent a biologically meaningful neuroprotective response rather than a nonspecific reduction in cellular stress.

In the present study, we integrated human AD transcriptomic analysis with experimental neuronal validation to identify and characterize disease-associated molecular candidates. Eleven candidate genes were initially prioritized from AD versus control (AD vs Control) transcriptomic datasets, of which APH-1A and CDK5 were experimentally validated and correlated by real time-quantitative polymerase chain reaction (RT-qPCR) following STZ exposure in SH-SY5Y cells. We subsequently used p-Tau_Ser396 as a disease-relevant molecular phenotype and combined confocal fluorescence imaging with AFM-based cellular morphological analysis to characterize STZ-induced neuronal alterations. Finally, we investigated whether Brahmi and Donep-M could attenuate the STZ-associated pathological phenotype. We hypothesized that transcriptome-derived APH-1A and CDK5 signatures would be responsive to AD-like neuronal stress and that pharmacological or phytochemicals intervention would reduce associated tau Ser396 phosphorylation and cellular structural abnormalities. This integrated transcriptomic to cellular strategy provides a framework for connecting human AD molecular signatures with experimentally measurable neuronal phenotypes and for evaluating potential therapeutic interventions.

Methodology

1. Identification of Alzheimer's disease related biomarkers via protein-protein interaction and hub proteins

The search keywords "Alzheimer's disease" was applied to find the common genes from databases which are available online, including Genecards (https://www.genecards.org/)(Safran et al. 2021), Comparative Toxicogenomics Database (CTD) (https://ctdbase.org/)(A. P. Davis et al. 2025) and OpenTargets (https://platform.opentargets.org/) and GSE33000(Narayanan et al. 2014), a transcriptomic dataset for AD pathology with respect to control was selected from the Gene Expression Omnibus database (GEO)(Cowan et al. 2010; S. Davis and Meltzer 2007). Genes satisfying adjusted P value (adj. $p < 0.05$) were considered statistically significant differentially expressed genes (DEGs). Positive (log2FoldChange) values of genes were classified as upregulated in AD, whereas genes with negative (log2FoldChange) values were classified as downregulated. The resulting significant gene list was subsequently used for candidate prioritization. DEGs (Smyth 2004; Ritchie et al. 2015) in AD vs control were represented with volcano plot. Using the Cytohubba(Chin et al. 2014) plugins in Cytoscape v3.10.4(Shannon et al. 2003), the top 20 hub genes were identified by importing the PPI network of common genes identified among AD and Primary cilia into Cytoscape v3.10.4. Common proteins (812) curated by mentioned above online databases were selected for GO (Gene ontology)(Carbon et al. 2021), including various components (cellular, biological and molecular functions), and signaling pathway analysis, which included KEGG(Kanehisa et al. 2021), WikiPathways(Martens et al. 2021), Reactome Pathways(Jassal et al. 2019), was performed using the ClueGo(Bindea et al. 2009) plugin of Cytoscape. The selected markers are highlighted in dot green to correlate AD and primary cilia biology.

2. Extraction of Brahmi by ethanol method

The extraction procedure was adapted from the standard protocols(Sumathi *et al.*, 2002; Phrompittayarat *et al.*, 2007) and optimised on laboratory conditions. Thirty grams of the coarsely ground Brahmi powder were soaked in a conical flask containing 300 ml of Milli-Q water at room temperature (RT) for 24 hrs. After 24 hrs, the soaked plant material was squeezed through a muslin cloth to produce an aqueous extract. The remaining plant material was subjected to percolation using 200 ml of 95% ethanol for three days at RT. The flask was sealed with aluminium foil containing small holes to minimise contamination and evaporation of the solvent. The extract was filtered through Whatman No.1 filter paper after three days. Approximately 150 ml of filtered extract was collected. Brahmi extract containing ethanol was evaporated by rotary evaporator using reduced pressure. The temperature of the water bath was maintained to 55°C, and the speed of rotation was set to between 90 rpm. The remaining 10 ml extract was lyophilised (high vacuum <0.1 mbar and at -59°C) to get dried Brahmi extract. The lyophilised extract was carefully transferred into airtight containers and stored at 4°C for subsequent use.

3. Mammalian Cell Culture and treatment conditions

SH-SY5Y (human neuroblastoma) cell line used for experimental study. The cells passage number 12 from frozen cryovial were revived by thawing at 37°C in a water bath for 2-3 min. The cells were mixed with pre-warmed complete media (DMEM:F12) supplemented with 10% FBS and 1% penicillin-streptomycin (PS) and centrifuged at 1000 rpm for 3 min. The supernatant was discarded to remove residual DMSO and cell pellets were then re-suspended into 6 ml

of complete media, followed by equal distribution of 3 ml each into two T-25 flasks. The cells were cultured and maintained under humidified conditions at a temperature of 37°C and 5% CO2. Subsequently, 500 µl of 1X trypsin-EDTA solution was added to the culture of T25 flask and incubated for 1-2 minute for detachment. The detached cells were wash with 1X phosphate-buffered saline (1X PBS) and gently resuspended in 1 ml of complete media. Cells were counted with hemocytometer and 0.3x 10^5 cells were seeded into 6 well plates for all experiments and 0.1x 10^5 cells for AFM study.

4. Development of Alzheimer's model using STZ in SH-SY5Y cell line

0.3x 10^5 SH-SY5Y cells at passage 14 were seeded onto sterile in 6-well culture plates and allowed to grow until they reached 50% confluency before treatment. SH-SY5Y cells with STZ at a final concentration of 5 mM for 24 hrs were treated. Following STZ treatment, cells were washed with 1X PBS to remove excess STZ and processed further treatment with Brahmi and anti-AD drugs.

5. Cell viability assay of STZ induced SH-SY5Y cells treated with Brahmi and anti-AD drugs

STZ exposed neuronal cells were treated with Brahmi (100 µM) and anti-AD drugs, Donep-M (100 µM) for 24hrs separately and in combination of both to observe their potential efficacy. MTT (3-(4,5-dimethylthiazol-2-yl)-2,5-diphenyltetrazolium bromide) assay was performed to measure cell viability. The preparation of stock solution of MTT for the experiment was followed by dissolving 5mg of MTT in 1 ml of 1X PBS. The reagent was vortexed for a uniform mixture and filtered with 0.2µm syringe filter to avoid any contamination. The modern anti-AD drug "Donep-M-10mg" composed of memantine hydrochloride (5mg) and donepezil hydrochloride (5mg), purchased from pharmacy, was dissolved into sterile Milli-Q water and filtered using 0.2µM syringe filter before treating cells. Further, media was removed from the cells that were previously added in a 96-well plate containing 0.5x10^4 cells per well in triplicate for each biological replicate. The final concentration of 0.5mg/ml MTT was used for cells viability measurement. After adding MTT, the cells were kept in a CO_2 incubator for 4 hrs. After 4 hrs, purple formazan crystals were formed and further dissolved by adding 150 µL of dimethyl sulfoxide (DMSO) was pipetted into each well of a 96-well plate. The plates were gently mixed to ensure complete dissolution of the formazan. The absorbance of each sample was taken at 590 nm in a plate reader (Varioskan™ LUX Multimode Microplate Reader, Thermo Scientific™). The percentage of viable cells of the sample was calculated with the control group by normalizing with blank and using the following to the formula:

$$Cell\ viability(\%) = \frac{Absorbance\ of\ (cell\ treated - blank)}{Absorbance\ of\ (untreated\ cell\ as\ a\ control - blank)} X\ 100$$

6. RNA Isolation, cDNA synthesis and qRT-PCR for targeted genes validation

Total RNA was isolated from the treated and non-treated group using the TRIzol method following the standard protocol (Chomczynski & Sacchi, 1987). Cells that were seeded in a 6-well plate were first gently rinsed with 1 ml of cold 1X PBS to remove the serum residue. After that, 1 ml TRIzol was pipetted into each well and cells were scraped using a sterile cell scraper. It was transferred in 1.5 ml micro-centrifuge tube (MCT) and kept at RT for 5-10min in

TRIzol and with 200µl of chloroform was mixed vigorously for 15-30 sec. The sample was again kept at RT for 10min following centrifugation at 13000 rpm for 15 min at 4°C. The RNA containing upper aqueous layer without disturbing interphase was carefully pipetted into a nuclease free MCT and 500µl of isopropanol was added to it, and the tube was inverted 10-15 times. After this, it was kept on ice for 30 min and centrifuged at 13000rpm at 4°C. After discarding the supernatant carefully, the pellet was washed with 1 ml of 75% molecular grade ethanol three times. The final residual ethanol was dried up at RT and pellet was resuspended in 20µl of DEPC treated water and kept for 10 min at 55°C. The concentration was determined via nanodrop and stored at -80°C.

For synthesis of complementary DNA (cDNA), the protocol of Verso cDNA Synthesis Kit, Thermo Fisher Scientific (USA) was followed carefully. The cDNA synthesised was stored at -20°C until it was used for quantitative PCR analysis. For gene expression analysis by qRT-PCR (QuantStudio5, Applied Biosystem), 5 ul of SYBR Green (Applied Biosystems SYBR Green Master Mix, Cat. No. A25742, Thermo Fisher Scientific, USA) was used in total 10ul reaction followed by 1ul of cDNA (1:10 diuted), 500nM of each primers and nuclease free water to make up 10ul reaction volume. The sequences of primers used for RT-qPCR are: APH-1A (Forward-5'-TCCATGGAGACTCACCCTATTA-3' and Reverse-5'-CAGGCATCAAAGAACACAACTC-3') and CDK5 (Forward-5'-GCGATGCAGAAATACGAGAAAC-3' and Reverse-5'-GTTTCAGAGCCACGATCTCAT-3'). The experimental condition for qRT-PCR was used default of the system with annealing at 60°C for all. The CT value of treated and non-treated was normalised to GAPDH's CT value and fold change was calculated using the $2^{-\Delta\Delta CT}$ method. Fold chamge has been calculated using following method:

$$\Delta CT = CT_{\text{Target}} / CT_{\text{non-target}} - CT_{GAPDH}$$

$$\Delta\Delta CT = CT_{\text{Target Gene}} - CT_{\text{non-target}}$$

$$\text{Fold change} = 2^{-\Delta\Delta CT}$$

7. Imaging of SH-SY5Y cells using Atomic force microscopy (AFM)

The surface architecture and the transformation of SH-SY5Y cell membrane upon exposure to SH-SY5Y cells with STZ (5mM), STZ treated cells with Brahmi (100µM), STZ treated cells with Donep-M (100µM) and STZ treated cells with both Brahmi and Donep-M were observed with an AFM, which consisted an AFM scanner and WITec alpha300 Raman microscope (Oxford Instruments witec360, Ulm, Germany). The structural transition of differentiated SH-SY5Ycells due to the exposure of STZ treated with or without Brahmi and Donep-M and the untreated cells as a control were visualized in the AFM. The cells were fixed with 4% PFA for 10 min and dried at RT and imaged with a monolithic silicon AFM probe aluminium-coated (30nm thick) cantilever with a resonance frequency and force constant of 300±100 kHz and 40±20 newtons/m, respectively, in non-contact and tapping mode operation (Tap300AI-G, BudgetSensors, Bulgaria). All images for were taken at a high resolution at a fixed scan speed of 0.5 second per line. All images were processed with witec360 software.

8. Immunocytochemistry of STZ induced and co-treated SH-SY5Y cells with Brahmi and Modern drugs to understand Alzheimer's disease pathology.

0.3x 10^5 SH-SY5Y cells were pipetted onto sterile coverslip placed in 6 well culture plates. STZ of 5mM was treated at 50% confluency. After 24 of treatment, 1x PBS was used for washing cells and were fixed with 4% formalin solution for 10 min at RT. Following fixation, cells were treated with 0.7% Triton X-100 in 1X PBS for 15 min to facilitate permeabilization for antibody penetration. Cells were incubated with 2% bovine serum albumin (BSA) in 1X PBS for 2 hrs at RT to block non-specific binding. To confirm the development of Alzheimer-like pathology, tau was assessed using immunocytochemistry. Cells were incubated overnight at 4°C with an anti-p-Tau_Ser396 polyclonal antibody (*Affinity, #Cat: AF3148*) diluted in 1X PBS containing 0.1% BSA. Cells were then incubated with Alexa 546™-tagged secondary antibody (*Thermo, #Cat: A11010*) for 1hr at RT in the dark. Nuclei were counterstained with DAPI mountant media (*ProLong Gold Antifade Mountant with DNA Stain DAPI, #Cat: P36931*) before imaging. The fluorescence images were visualized and acquired using a *Nikon ECLIPSE Ti Series* confocal microscope operating at a 60x magnification using oil immersion. After capturing these images, the relative intensity was calculated using Fiji-Image J software with a minimum of $n \geq 30$ cells per group.

Statistical analysis

The graphs representing data show mean ± SEM. For statistical significance analysis, one way ANOVA was performed using GraphPad Prism 8 where * $p < 0.05$, ** $p < 0.01$, and *** $p < 0.001$ represent significant differences; ns = non-significant with respect to control and between the treatment groups.

Results

1. Integrative systems biology identifies hub genes associated with Alzheimer's disease

Common genes (7818) associated with AD were identified after filtering out the duplicate genes from GeneCards (20,190 genes), OpenTargets (13,367 genes), Comparative Toxicogenomics Database (CTD) (27,328 genes), and GSE33000 (AD vs control; 15,854 genes) datasets **(Figure. 1A)** (see supplementary Excel sheets 1–4). Importantly, transcriptomic analyses of human AD brain tissue have identified substantial alterations in genes associated with primary-cilium structure and function(Kobayashi et al. 2022; E. Miller et al. 2024; Yeo et al. 2023). In the present study, it has also been found that there are several common markers associated between AD and PD (Parkinson's disease) **(Fig.SI 1A)**. Subsequently, we also elucidated the common genes associated among AD, PD and Primary ciliary complex to understand the betweenness and correlate among neurodegenerative disorders like AD, PD and neural cilia. It was found 811 common genes represented via Venn-diagram **(Fig.SI 1A)**. Further, to identify molecular candidates potentially linking AD pathology with primary cilium dysfunction in our current study, a protein-protein interaction (PPI) network analysis of genes associated with AD and the primary ciliary complex was performed (Fig.S1B) and majorly involved ciliary complex genes. The top 20 genes were selected via PPI between AD and ciliary complex, and based on ranking algorithm of *BottleNeck* score, GAPDH and IFT57 had the highest, being the major connectors of both major clusters in the network. The above cluster involved the genes related to AD, like APOE, PSEN1, ADAM10, **ADAM17** and **CDK5**. The lower cluster of this interactome primarily contains ciliary genes like IFTs, TTC8, BBS2, MKS1, CLUAP1, and ARL6 that are involved in cilia formation and intracellular transport. (Figure. 1B, S1B and S1G). Differentially expressed genes (DEGs) were considered in the gene expression dataset GSE33000 for AD vs control based on a false discovery rate (FDR) corrected p-value <0.05 and Log2Fold Change ≥ 0 and < 0. (Fig.1C) and DEGs of Parkinson's disease and primary ciliary complex were also shown in volcano plots (Fig.S1C, S1D and S1E; see supplementary Excel sheets 5-6). The upregulated and downregulated DEGs were detected separately for GSE33000 and genes annotated in green are the markers selected for experimental validation due to their association with common to both AD (ADAM17, APH-1A, MAPT, CDK5, and PSEN2) and primary cilia (CLUAP1, IFT20, IFT57, IFT80, IFT88 and IFT172) (refer supplementary excel sheets S4-S5). The 811 common genes among AD, PD and primary cilia identified from the databases were exported to Cytoscape for network analysis via String v12.0 (https://string-db.org/)(Szklarczyk et al. 2023) using multiprotein search domain for protein-protein interaction (PPI) analysis. The PPI network was constructed (Fig.SI1F). The plugin of Cytoscape (ClueGO) was utilized for gene ontology (GO) (biological process, cellular component, and molecular function) and pathway (KEGG, WikiPathways, and Reactome) analysis of 811 common genes (Fig.SI2).

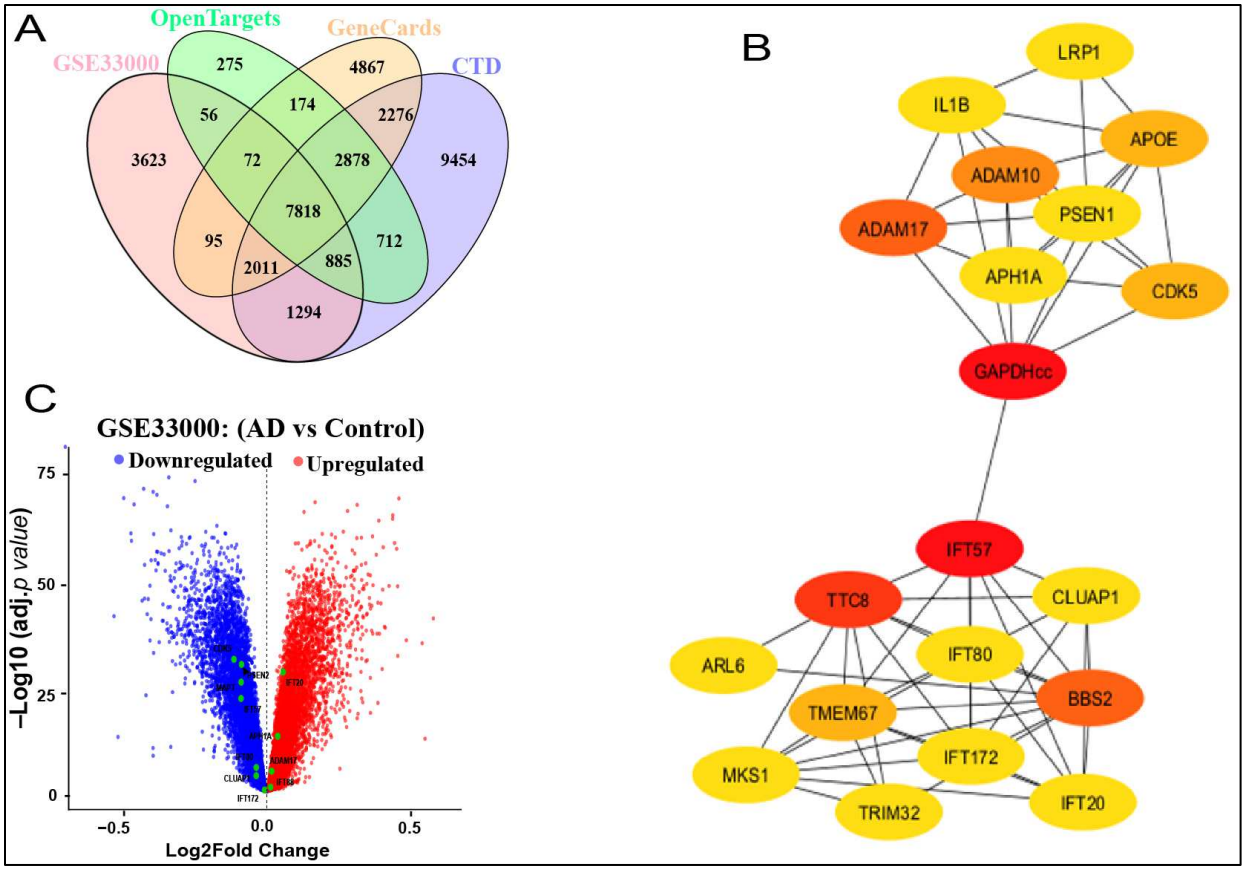


Fig.1. Identification of transcriptomic derived candidates to Alzheimer's disease. (A) Venn-diagram showing common genes (7818) associated with AD identified from OpenTargets, GeneCards, the Comparative Toxicogenomics Database (CTD), and GSE33000 (AD vs Control) online databases. (B) Top 20 hub genes identified via cytohubba plugin of Cytoscape 3.10.4. (C) Volcano plot depicting DEGs of GSE33000 (AD vs Control) represented in dot red are significantly upregulated and downregulated genes are in dot blue colour associated with AD. Highlighted with annotation in green are markers selected (ADAM17, APH-1A, MAPT, CDK5, PSEN2, CLUAP1, IFT20, IFT57, IFT80, IFT88 and IFT172) in association of AD pathology.

2. Brahmi and Donep-M enhanced SH-SY5Y cells' viability under STZ induced stress

Initially, the extracts of Brahmi were characterized via UV-spectrophotometer (Fig.SI3A), gas chromatography-mass spectrophotometer (GC-MS) (Fig.SI 3B) and liquid chromatography-mass spectrophotometer (LC-MS) (Fig.SI3C) in order to confirm its constituents. The compositions of Brahmi were analysed from their respective chromatograms and listed in tables (refer SI tables I-III). Following confirmation of phytochemicals, the effect of Brahmi, Donep-M, and STZ on the SH-SY5Y cells' viability were tested and evaluated using MTT assay. Our result indicate that STZ (1mM, 2.5mM, 5mM and 10mM) significantly reduced the number of viable cells at 24hrs treatment on increasing dose with respect to control (non-treated cells) **(Fig.2A)**. Similarly, Brahmi at concentration (25 µM, 50 µM, 75 µM,

100 µM, and 200 µM) reduced the number of viable cells 24hrs of treatment in a dose-dependent manner compared to control cells with highest cell viability at 100 µM **(Fig.2B)**, whereas the cells treated with Donep-M at concentration (50 µM, 100 µM and 200 µM) we found to be significantly non-toxic **(Fig.2C)**. Subsequently, in STZ (5mM) treated cells, treatment of Brahmi and Donep-M at varying concentration (50 µM, 100 µM and 200 µM) separately for 24hrs resulted in the optimal cell viability at 100 µM in both cases, which shows that Brahmi and Donep-M at 100 µM significantly inhibited the toxic effects of STZ as shown in **Fig.2D&E**. Our results indicate that Brahmi and modern anti-AD drugs are safe to explore for their synergistic potential on in-vitro AD model system.

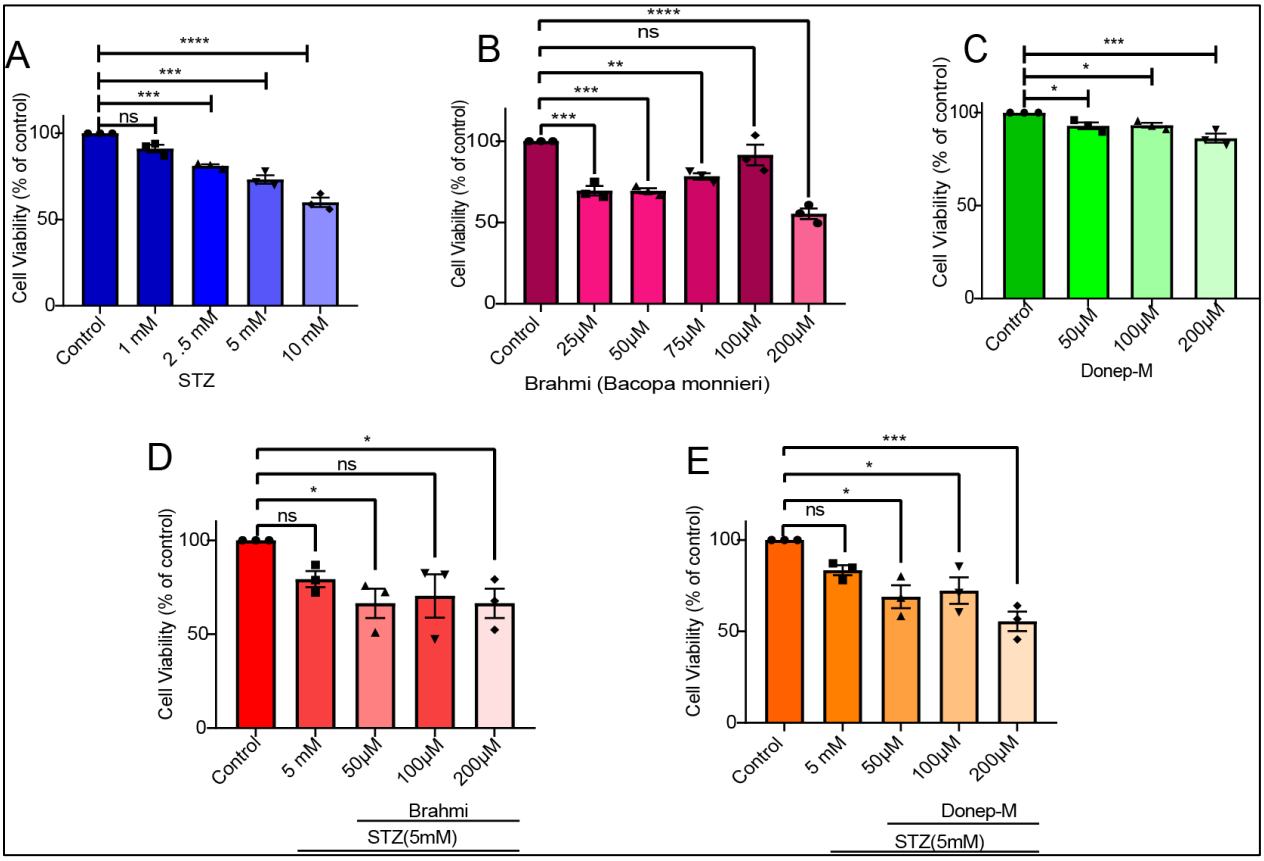
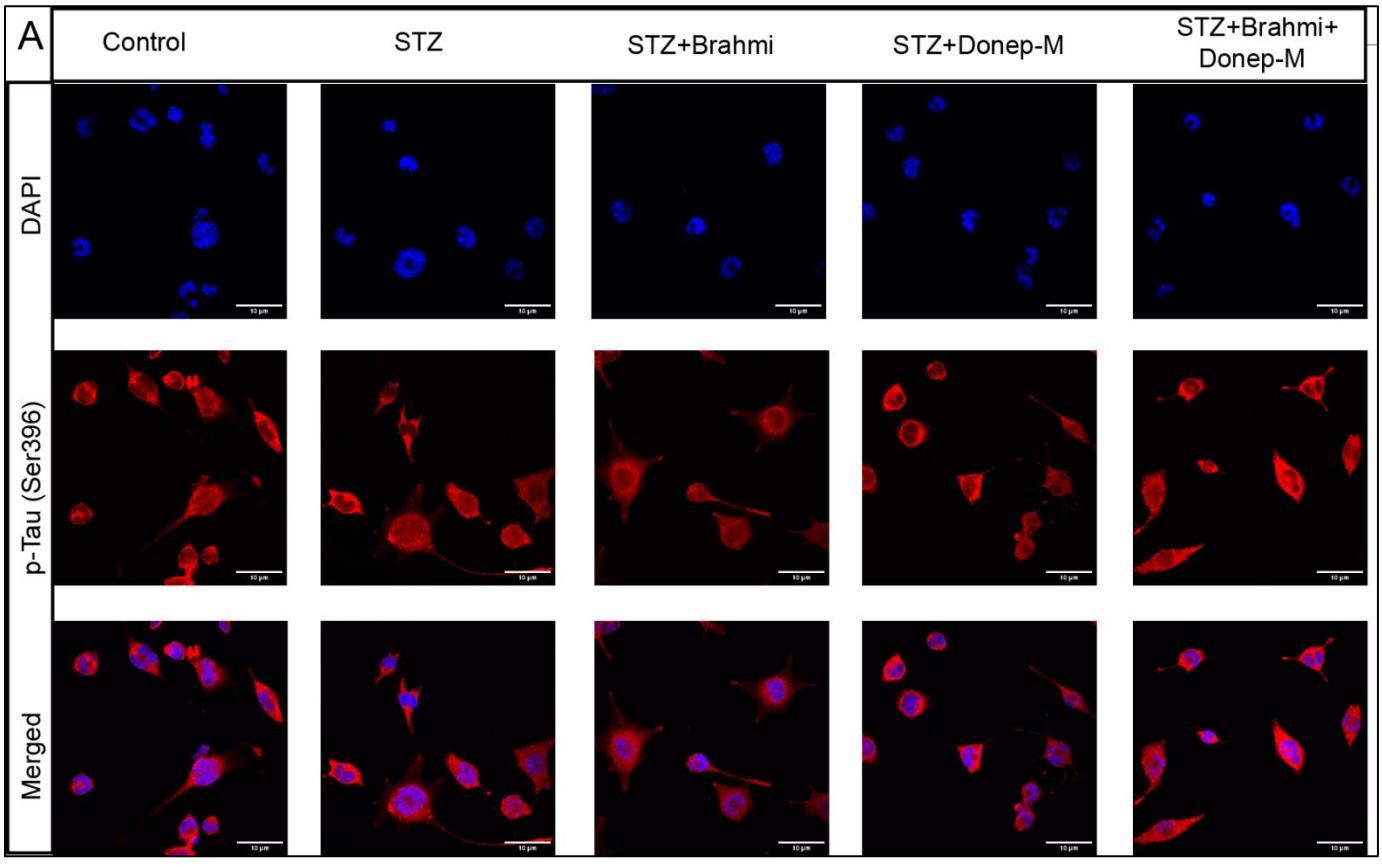


Fig.2. MTT assay for SH-SY5Y cells viability after **(A)** streptozotocin (STZ) treatment (1mM, 2.5mM, 5mM and 10mM), **(B)** Brahmi treatment (25 µM, 50 µM, 75 µM, 100 µM, and 200 µM), **(C)** Donep-M (Memantine and Doenepzil) treatment (50 µM, 100 µM, and 200 µM), and STZ (5mM) treated cells with **(D)** Brahmi and **(E)** Donep-M at different concentration (50 µM, 100 µM, and 200 µM). The Y-axis represents the percentage of cell viability with respect to control whereas X-axis denotes the concentration of STZ, Brahmi and Donep-M. The data represented using bar graph showing mean ± SEM. One way ANOVA was performed using GraphPad Prism 8. * $p < 0.05$, ** $p < 0.01$, and *** $p < 0.001$ represent significant differences; ns = non-significant with respect to control and between the treatment groups.

3. Brahmi and Donep-M reduces Tau phosphorylation

AD pathology is characterized by the post-translational modifications of Tau known as phosphorylation, which ultimately leads to its toxicity. There are 85 phosphorylation sites reported which are targeted by various kinases. To evaluate Tau associated pathology in the STZ induced in in-vitro model, p-Tau_Ser396 immunoreactivity was examined in SH-SY5Y cells using confocal fluorescence microscopy. Compared with untreated control cells, STZ treated cells exhibited a marked increase in p-Tau_ Ser396 fluorescence intensity, indicating enhanced accumulation of the Ser396-phosphorylated Tau epitope following STZ induced neuronal stress via quantitative image analysis. Importantly, co-treatment with Brahmi and Donep-M reduced and increased p-Tau_Ser396 fluorescence relative to STZ treated cells and untreated control cells respectively. Similarly, co-treatment with Brahmi and the anti-Alzheimer's drugs (Donep-M) together significantly attenuated the STZ associated increase in p-Tau_Ser396 immunoreactivity **(Fig.3A&B)**. The reduced fluorescence signal following these interventions indicates attenuation of the pathological Tau phosphorylation phenotype induced by STZ. Collectively, these findings demonstrate that the STZ treated SH-SY5Y model exhibits increased p-Tau_Ser396 associated pathology and that this phenotype is responsive to both Brahmi and established pharmacological interventions.



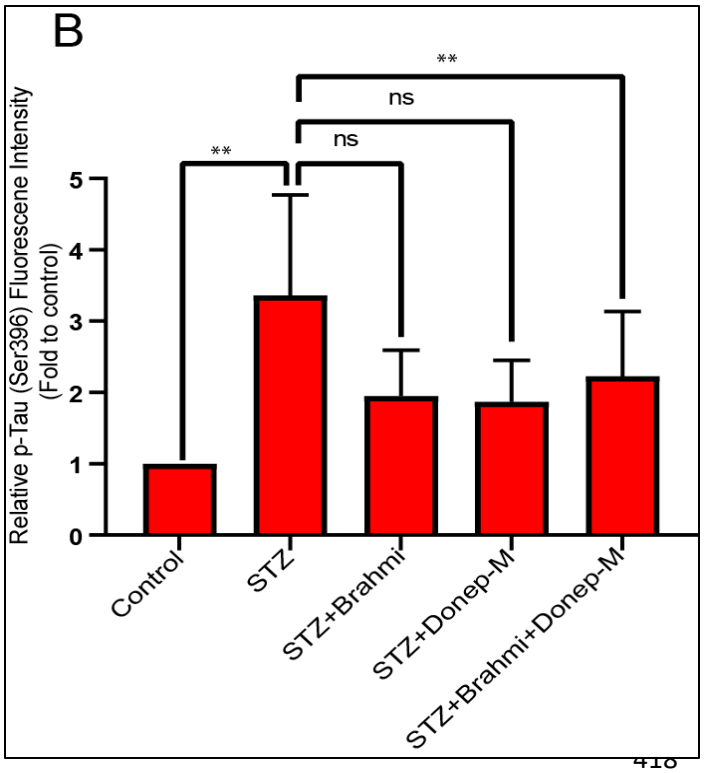


Fig.3. Brahmi and Donep-M attenuate Tau hyperphosphorylation. (A) Confocal microscopy immunofluorescence images. Scale bar represents 10µm. (B) Quantification of phospho-Tau fluorescence in STZ treated cells and co-treatment with Brahmi and Donep-M. The analysis of images were processed using Fiji-Image J software. The data represented using bar graph showing mean ± SEM. One way ANOVA was performed using GraphPad Prism 8. * $p < 0.05$, ** $p < 0.01$, and *** $p < 0.001$ represent significant differences; ns = non-significant with respect to control and between the treatment groups.

4. Brahmi and Donep-M treatment establish membrane integrity in STZ induced cells

The cytoskeleton of neuronal cell constitute of microtubules, actin filament, and neuro-filaments, which are essential for plasticity, polarity, morphology, and integrity of neurons (Kevenaar and Hoogenraad 2015). However, amyloid in many neurodegenerative conditions, has altered the cytoskeleton due to its accumulation in cells (Mokhtar et al. 2013). It has been also reported that STZ treated neuronal cells has condition of amyloid plaque aggregation leading to oxidative stress and neurodegenerative disease like pathology(Biswas et al. 2016). Our result implicate transformation of membrane surface upon STZ treatment of neuronal SH-SY5Y cells **(Fig.4A&4B).** Further, to observe the reverse transformation or restoration of surface architecture of STZ treated cells, we treated the cells with Brahmi and Donep-M separately and together. STZ treated cells' surface morphology were disrupted in comparison to untreated control and treated with Brahmi and Donep-M drug. Our results strongly suggest that, STZ treated cells with Brahmi in

combination with Donep-M has synergistic effect on restoring the morphology of neuronal cells evidenced by line profile height **(Fig.4C)** and also have potential for treating neurodegenerative disease conditions.

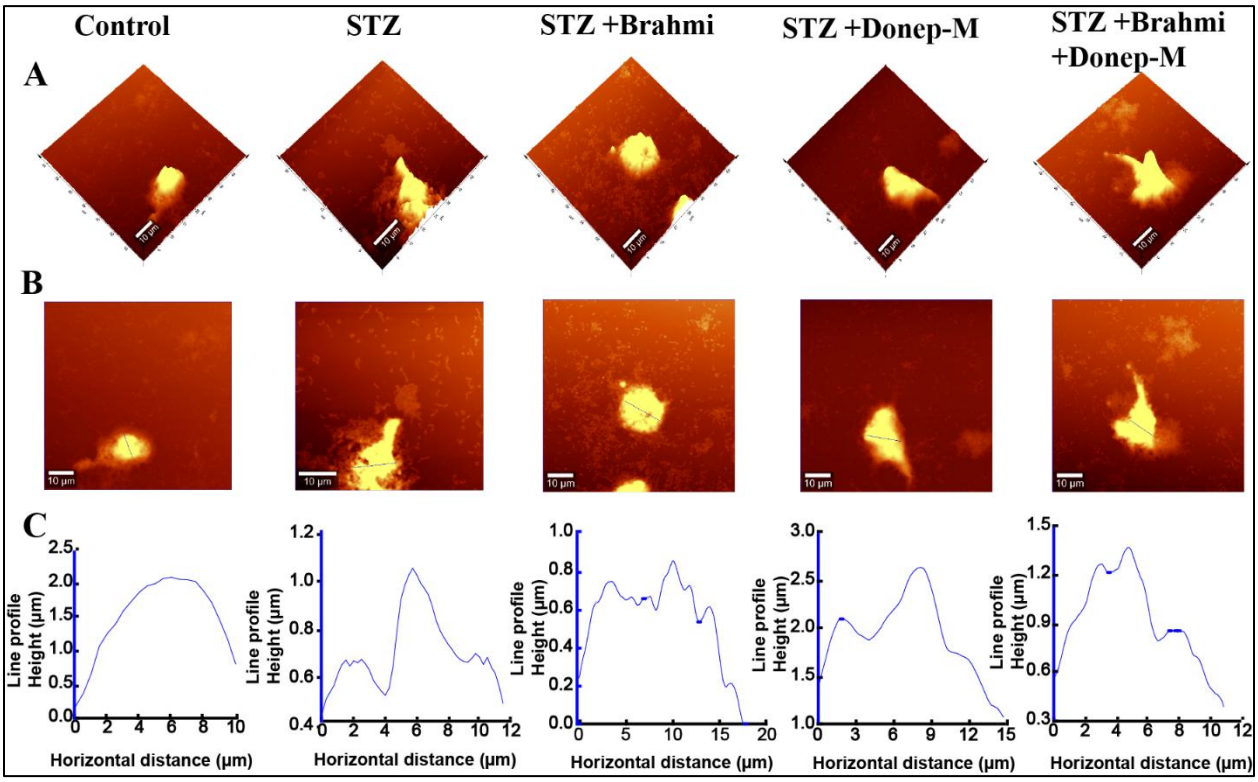


Fig.4. Analysis of surface morphology in SH-SY5Y cells by STZ treatment along with Brahmi and modern anti-AD drugs. SH-SY5Y cells were exposed with 5mM STZ, 100µM Brahmi and 100µM modern anti-AD drugs (Donep-M) for 24hrs. **A.** Three-dimensional (3-D) AFM images (60 × 60 µm) of SH-SY5Y cells. **B.** Two-dimensional (2-D) height image of SH-SY5Y cells represented by a line across the border of cell surface to evaluate surface smoothness. STZ-treated cells possess distorted membrane of SH-SY5Y cells. **C.** Cross sectional profile for the various conditions of SH-SY5Y cells suggest that the most affected surface morphology across STZ-treated cells.

5. Experimental validation by mRNA expression level of APH-1A and CDK5

To obtain a biologically relevant set of AD associated molecular candidates for experimental validation, the significant DEG list was subjected to candidate prioritization. Candidate genes were selected based on their association with AD related molecular pathways, neuronal function, protein processing, intracellular signaling, cytoskeletal regulation, and/or previously reported links to neurodegenerative disease linking to primary cilia because primary cilia are reported to be associated with neurodegenerative disease like AD(Guo et al. 2025; Kobayashi et al. 2022; Mokhtar et al. 2013). Out of eleven candidate genes, APH-1A and CDK5 demonstrated reproducible expression changes following STZ treatment with Brahmi and co-treatment with Brahmi and Donep-M. Our gene expression analysis of APH-1A in STZ treated cells is upregulated by ~0.5 fold change and ~0.8 fold change in comparison to control and

Brahmi treated experiments respectively, whereas downregulated by ~0.3 fold change in comparison to Donep-M alone and co-treatment with Brahmi and Donep-M. On other side, CDK5's expression in STZ treated cells is upregulated by ~0.5 fold change with respect to control, Brahmi and co-treated with Brahmi and Donep-M together but ~0.3 fold change upregulated to Donep-M treated cells. Further, molecular docking was performed of APH-1A (Fig.SI4) and CDK5 (Fig.SI5) with phytochemicals of Brahmi to understand and correlate the binding efficiency of metabolites. The docking results predicted the Stigmasterol as a best pose with APH-1A having least binding affinity of -10.9 (see SI table IV) whereas Bacoside B as a best pose with CDK5 having least binding affinity of -9.5 (see SI table V). Our transcriptomics and experimental approach enabled the identification of APH-1A and CDK5 as an AD associated candidate genes, which were subsequently investigated in relation to tau pathology and treatment associated phenotypic changes supported the evidence with the results of molecular docking. Therefore APH-1A and CDK5 need to be selected for further investigation in relation to AD associated neuronal pathology and therapeutic modulation.

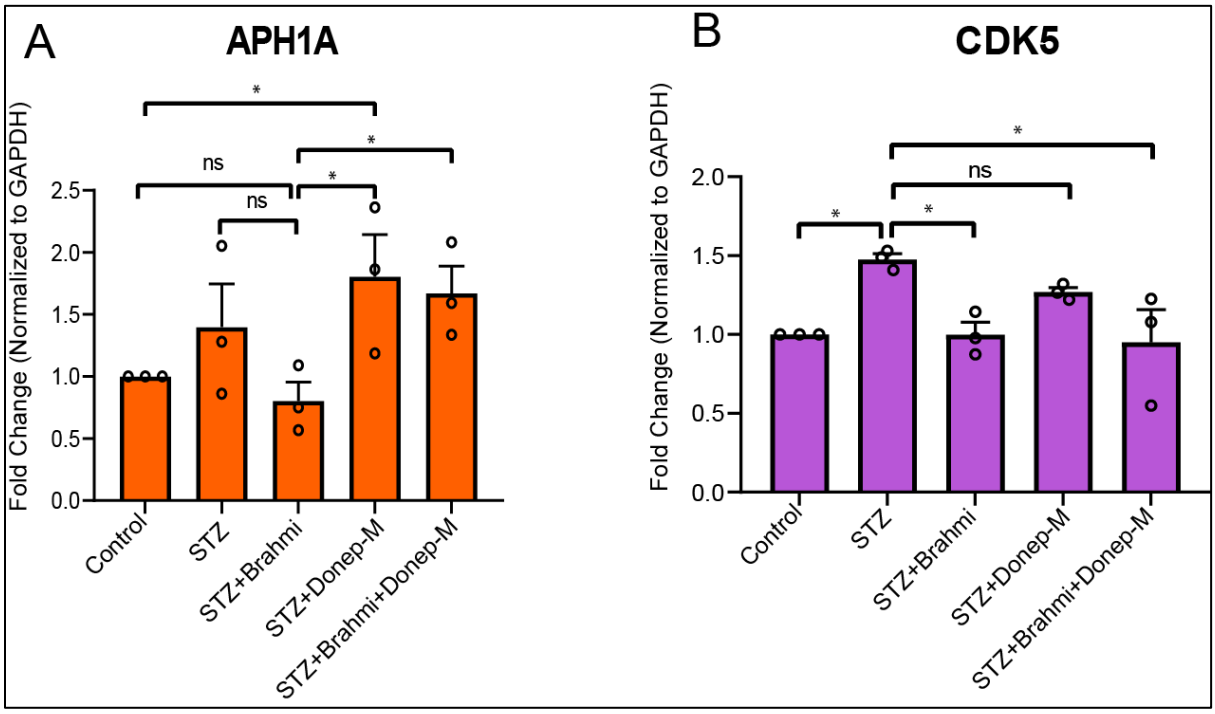


Fig.5. Gene expression analysis validation of transcriptomic derived AD markers by RT-qPCR (A) APH-1A and **(B)** CDK5. The data represented using bar graph showing mean ± SEM. One way ANOVA was performed using GraphPad Prism 8. * $p < 0.05$, ** $p < 0.01$, and *** $p < 0.001$ represent significant differences; ns = non-significant with respect to control and between the treatment groups. (n=3 in each biological replicates of 3)

Discussion

An integrated transcriptomic and experimental cellular strategy to identify and validate molecular alterations associated with human AD pathology will be useful for evaluating potential therapeutic interventions. Initially interrogating AD vs control transcriptomic datasets, we prioritized eleven candidate genes focused on AD pathology and their co-relation with cilia biology and subsequently tested their responsiveness in an experimentally STZ induced

neuronal model. Among these candidates, APH-1A and CDK5 showed reproducible expression changes following STZ exposure in SH-SY5Y cells, providing experimental support for their association with AD like neuronal pathology. In particular, the molecular findings were complemented by phenotypic characterization of tau pathology using confocal microscopy and AFM. STZ exposure was associated with increased phosphorylation of tau at Ser396, whereas co-treatment with Brahmi and Donep-M attenuated this pathological phenotype. Together, our findings connect AD associated transcriptional biomarkers with experimentally measurable neuronal and tau-related phenotypes.

Majorly, the reduction of p-Tau_Ser396 following Brahmi co-treatment represents an important therapeutic component of the present study. Brahmi has attracted considerable interest as a neuroprotective botanical because its bioactive constituents have been associated with antioxidant, anti-inflammatory, and anti-amyloid/tau-related activities(Sushma et al. 2024; Dubey et al. 2023). Experimental evidence has directly demonstrated that Brahmi's extract can inhibit tau aggregation and reduce pathological tau phosphorylation in neuronal cells(Dubey et al. 2023). Dubey et al. reported that Brahmi reduced phospho-tau accumulation and GSK3β phosphorylation in a cellular model of tau-associated stress, while also reducing oxidative and apoptotic responses. Our findings are consistent with these observations but extend them in an important direction. Whereas previous work investigated Brahmi in tau-stressed neuronal cells, our study evaluates its effect in a transcriptome-guided STZ-induced neuronal model in which APH-1A and CDK5 were independently validated as AD-associated candidates. Moreover, the reduction in p-Tau Ser396 observed after Brahmi co-treatment provides evidence that the phytochemical intervention can attenuate a disease-relevant tau phenotype in this cellular context.

Recent in-vivo work further supports the anti-tau potential of Brahmi where an Aβ42-induced AD model, Brahmi administration reduced pathological increases in phospho-tau and total tau and was associated with modulation of mitochondrial dysfunction and GSK3β/Wnt/β-catenin signaling(Sushma et al. 2024). These findings, together with our cellular results, suggest that the effects of Brahmi on tau pathology may involve multiple converging mechanisms rather than a single molecular target. Nevertheless, the present study does not establish which phytochemical constituent is responsible for the observed response but our molecular docking results predict Stigmasterol and Bacoside B as best poses with least binding affinity with APH-1A and CDK5 respectively. Future studies incorporating chemically characterized fractions or purified Stigmasterol or Bacosides B will therefore be required to identify the active component(s). Subsequently, The reduction of p-Tau_Ser396 following co-treatment with Donep-M, anti-AD drugs, provides an important pharmacological reference for interpreting the effect of Brahmi. Including established anti-AD agents allows the response to Brahmi to be evaluated against interventions with recognized clinical use rather than against untreated controls alone. The observation that both conventional drugs and Brahmi reduced the pathological tau phenotype suggests that the STZ-induced model is responsive to pharmacological modulation. However, memantine and donepezil have distinct primary pharmacological actions and should not be considered direct tau-targeting agents. Memantine primarily modulates NMDA receptor-mediated glutamatergic signaling, whereas donepezil inhibits acetylcholinesterase and enhances cholinergic neurotransmission(Guler et al. 2024). Therefore, the reduction of p-Tau Ser396 following these treatments may represent an indirect consequence of

improved cellular signaling, reduced excitotoxicity or metabolic stress, or broader neuroprotective effects. Consequently, the present results support the use of these drugs as pharmacological comparators rather than implying that their primary mechanism is inhibition of tau phosphorylation.

As a major strength of transcriptomic data was the starting point for candidate identification rather than selecting molecular targets solely on the basis of previously established AD pathways. Although transcriptomic analyses can reveal extensive molecular candidates associated with AD, individual DEGs require experimental validation because postmortem brain datasets are influenced by cellular heterogeneity, disease stage, tissue composition, and secondary responses to neurodegeneration(Hou et al. 2025; Shin et al. 2026). This observation emphasizes that changes in CDK5 and APH-1A expression should not automatically be interpreted as evidence of pathological association relating kinase activation. On the other hand, our molecular docking result suggests that Bacoposide 1 and Bacosaponin c does not take part in inhibiting the tau aggregation and it does not show inhibiting effect on the CDK5 although the docking score came around -7.5 to -9.19 (refer SI Fig.5 and table VI and VII) but experimentally, our study has shown the differential mRNA expression level of CDK5 and APH1A. Our finding reveals that APH-1A and CDK5 expression respond to STZ exposure therefore provides an experimentally relevant association that warrants further investigation at the protein activity level. The response of APH-1A and CDK5 to STZ exposure was accompanied by an increase in tau phosphorylation at Ser396, supporting the development of an AD-like neuronal phenotype in SH-SY5Y cells. STZ-treated neuronal cells have been studied experimentally to reproduce several features associated with AD-related cellular dysfunction, including oxidative stress, mitochondrial impairment, endoplasmic-reticulum stress, altered signaling pathways, and tau-associated abnormalities(Plaschke and Kopitz 2015; Bagaméry et al. 2021; Singh, Tiwari, and Singh 2024; Biswas et al. 2016). The increase in p-Tau Ser396 observed in our model is particularly relevant because tau hyperphosphorylation disrupts its physiological interaction with microtubules and contributes to cytoskeletal instability and pathological tau accumulation(Bramblett et al. 1993; T. Li and Paudel 2006; Gao et al. 2018; Neddens et al. 2018).

The selection of Ser396 as a pathological readout is also relevant because this site is among the established AD-associated phosphorylation sites of tau and can be influenced by multiple neuronal kinases, including CDK5 and GSK3-family kinases(T. Li and Paudel 2006; N. Miller et al. 2015; Vossel et al. 2015; Huang et al. 2017; Sushma et al. 2024; Fu et al. 2025). Importantly, the present findings should not be interpreted as demonstrating that the observed p-Tau_Ser396 increase is directly caused by altered CDK5 expression. Rather, the data demonstrate a concordant response of a transcriptome-derived candidate and a disease-relevant tau phenotype following STZ-induced neuronal stress. Demonstrating a direct CDK5-tau relationship in this model would require additional experiments involving CDK5 inhibition, knockdown, overexpression, kinase activity measurements, or rescue experiments. The increase in p-Tau_Ser396 detected by confocal microscopy provides an important phenotypic link between the transcriptomic findings and neuronal pathology. Fluorescence-based detection allows spatial assessment of pathological tau within individual cells and provides information that cannot be obtained from gene-expression measurements alone. Thus, the combination of RT-qPCR and confocal microscopy in the present study provides two complementary levels of evidence, transcriptional responsiveness at the candidate-gene level and pathological protein modification at the

cellular level. This distinction is important because changes in mRNA abundance do not necessarily predict changes in protein abundance, localization, post-translational modification, or cellular function.

An additional feature of the present study is the incorporation of AFM alongside confocal imaging. Conventional fluorescence microscopy primarily provides molecular and spatial information, whereas AFM can provide nanoscale topographical and biomechanical information from individual cells(Dague et al. 2022; Legleiter and Kowalewski, n.d.; Chen et al. 2023). This distinction is particularly relevant to AD because tau pathology is closely linked to disruption of the neuronal cytoskeleton and changes in cellular architecture(Gao et al. 2018). In the present study, the AFM observations associated with STZ treatment therefore provide a complementary dimension to the confocal p-Tau findings. Rather than treating increased p-Tau fluorescence as an isolated molecular event, the combination of confocal and AFM imaging allows tau-associated pathology to be considered in the context of broader cellular structural alterations.

Finally, future studies should therefore investigate whether manipulation of APH-1A or CDK5 directly modifies the STZ-induced p-Tau phenotype. CDK5 inhibition or knockdown, APH-1A knockdown/overexpression, measurement of CDK5 kinase activity, and assessment of γ-secretase activity and Aβ production would substantially strengthen the mechanistic interpretation(Tanaka et al. 2001; Ma et al. 2005; Zheng et al. 2005; Kimura, Ishiguro, and Hisanaga 2014; N. Miller et al. 2015; Vossel et al. 2015; Todd et al. 2022; Hernández-Hernández et al. 2025). It would also be valuable to determine whether the AFM phenotype correlates quantitatively with p-Tau Ser396 and cytoskeletal markers such as βIII-tubulin, MAP2, and F-actin(Nishida et al. 2023; Chen et al. 2023; Dague et al. 2022). For Brahmi, fractionation and characterization of individual bacosides could determine whether the observed neuroprotective effect is attributable to a specific constituent or to synergistic activity of the extract(Dubey et al. 2023; Sushma et al. 2024; Fatima et al. 2022).

Conclusion

In conclusion, this study provides a transcriptome-guided experimental framework for connecting AD-associated molecular signatures with neuronal pathology. APH-1A and CDK5 emerged from an initial panel of eleven candidates and were experimentally validated as STZ-responsive genes in SH-SY5Y cells. STZ exposure was accompanied by increased tau Ser396 phosphorylation and cellular structural alterations, while Brahmi, memantine, and donepezil attenuated the pathological tau phenotype. The integration of RT-qPCR, confocal microscopy, and AFM provides complementary molecular, spatial, and biophysical evidence of the neuronal response. Although further mechanistic studies are required to establish whether APH-1A or CDK5 directly drives tau pathology, the findings identify these genes as promising experimentally validated candidates and support Brahmi as a potential multi-target neuroprotective intervention worthy of further investigation in AD models.

References

Alonso, Alejandra del C., Inge Grundke-Iqbal, Héctor S. Barra, and Khalid Iqbal. 1997. "Abnormal Phosphorylation of Tau and the Mechanism of Alzheimer Neurofibrillary Degeneration: Sequestration of Microtubule-Associated Proteins 1 and 2 and the Disassembly of Microtubules by the Abnormal Tau." *Proceedings of the National Academy of Sciences* 94 (1): 298–303. https://doi.org/10.1073/pnas.94.1.298.

Bagaméry, Fruzsina, Kamilla Varga, Kitti Kecsmár, István Vincze, Éva Szökő, and Tamás Tábi. 2020. "Lack of Insulin Resistance in Response to Streptozotocin Treatment in Neuronal SH-SY5Y Cell Line." *Journal of Neural Transmission* 127 (1): 71–80. https://doi.org/10.1007/s00702-019-02118-5.

2021. "The Impact of Differentiation on Cytotoxicity and Insulin Sensitivity in Streptozotocin Treated SH-SY5Y Cells." *Neurochemical Research* 46 (6): 1350–58. https://doi.org/10.1007/s11064-021-03269-2.

Barthélemy, Nicolas R., Yan Li, Nelly Joseph-Mathurin, Brian A. Gordon, Jason Hassenstab, Tammie. L. S. Benzinger, Virginia Buckles, et al. 2020. "A Soluble Phosphorylated Tau Signature Links Tau, Amyloid and the Evolution of Stages of Dominantly Inherited Alzheimer's Disease." *Nature Medicine* 26 (3): 398–407. https://doi.org/10.1038/s41591-020-0781-z.

Barthélemy, Nicolas R., Benjamin Saef, Yan Li, Brian A. Gordon, Yingxin He, Kanta Horie, Erik Stomrud, et al. 2023. "CSF Tau Phosphorylation Occupancies at T217 and T205 Represent Improved Biomarkers of Amyloid and Tau Pathology in Alzheimer's Disease." *Nature Aging* 3 (4): 391–401. https://doi.org/10.1038/s43587-023-00380-7.

Basheer, Aneesh, Ayush Agarwal, Biswamohan Mishra, Anu Gupta, Madakasira Vasantha Padma Srivastava, Richard Kirubakaran, and Venugopalan Vishnu. 2022. "Use of Bacopa Monnieri in the Treatment of Dementia Due to Alzheimer Disease: Systematic Review of Randomized Controlled Trials." *Interactive Journal of Medical Research* 11 (2): e38542. https://doi.org/10.2196/38542.

Bindea, Gabriela, Bernhard Mlecnik, Hubert Hackl, Pornpimol Charoentong, Marie Tosolini, Amos Kirilovsky, Wolf-Herman Fridman, Franck Pagès, Zlatko Trajanoski, and Jérôme Galon. 2009. "ClueGO: A Cytoscape Plug-in to Decipher Functionally Grouped Gene Ontology and Pathway Annotation Networks." *Bioinformatics* 25 (8): 1091–93. https://doi.org/10.1093/bioinformatics/btp101.

Biswas, Joyshree, Poonam Goswami, Sonam Gupta, Neeraj Joshi, Chandishwar Nath, and Sarika Singh. 2016. "Streptozotocin Induced Neurotoxicity Involves Alzheimer's Related Pathological Markers: A Study on N2A Cells." *Molecular Neurobiology* 53 (5): 2794–2806. https://doi.org/10.1007/s12035-015-9144-z.

Braak, H., and E. Braak. 1991. "Neuropathological Stageing of Alzheimer-Related Changes." *Acta Neuropathologica* 82 (4): 239–59. https://doi.org/10.1007/BF00308809.

Bramblett, Gregory T., Michel Goedert, Ross Jakes, Sandra E. Merrick, John Q. Trojanowski, and Virginia M.Y. Lee. 1993. "Abnormal Tau Phosphorylation at Ser396 in Alzheimer's Disease Recapitulates Development and

Contributes to Reduced Microtubule Binding." *Neuron* 10 (6): 1089–99. https://doi.org/10.1016/0896-6273(93)90057-X.

Busche, Marc Aurel, and Bradley T. Hyman. 2020. "Synergy between Amyloid-β and Tau in Alzheimer's Disease." *Nature Neuroscience* 23 (10): 1183–93. https://doi.org/10.1038/s41593-020-0687-6.

Carbon, Seth, Eric Douglass, Benjamin M Good, Deepak R Unni, Nomi L Harris, Christopher J Mungall, Siddartha Basu, et al. 2021. "The Gene Ontology Resource: Enriching a GOld Mine." *Nucleic Acids Research* 49 (D1): D325–34. https://doi.org/10.1093/nar/gkaa1113.

Cavallini, Annalisa, Suzanne Brewerton, Amanda Bell, Samantha Sargent, Sarah Glover, Clare Hardy, Roger Moore, et al. 2013. "An Unbiased Approach to Identifying Tau Kinases That Phosphorylate Tau at Sites Associated with Alzheimer Disease." *Journal of Biological Chemistry* 288 (32): 23331–47. https://doi.org/10.1074/jbc.M113.463984.

Chen, Yujuan, Kaige Qu, Ying Wang, Qinghan Zhang, Ying Xie, and Zuobing Wang. 2023. "Study on Calceolarioside A Anti-Aβ 25–35 -Induced Damage in SH-SY5Y Cells by Atomic Force Microscopy." *Chemistry & Biodiversity* 20 (6). https://doi.org/10.1002/cbdv.202300430.

Chin, Chia-Hao, Shu-Hwa Chen, Hsin-Hung Wu, Chin-Wen Ho, Ming-Tat Ko, and Chung-Yen Lin. 2014. "CytoHubba: Identifying Hub Objects and Sub-Networks from Complex Interactome." *BMC Systems Biology* 8 (S4): S11. https://doi.org/10.1186/1752-0509-8-S4-S11.

Chongtham, Anjalika, Aarthi Ramakrishnan, Marissa Farinas, Diede W. M. Broekaart, Joon Ho Seo, Carolyn W. Zhu, Mary Sano, Li Shen, and Ana C. Pereira. 2025. "Neocortical Tau Propagation Is a Mediator of Clinical Heterogeneity in Alzheimer's Disease." *Molecular Psychiatry* 30 (9): 4194–4213. https://doi.org/10.1038/s41380-025-02998-y.

Cowan, Catherine M., Torsten Bossing, Anton Page, David Shepherd, and Amritpal Mudher. 2010. "Soluble Hyper-Phosphorylated Tau Causes Microtubule Breakdown and Functionally Compromises Normal Tau in Vivo." *Acta Neuropathologica* 120 (5): 593–604. https://doi.org/10.1007/s00401-010-0716-8.

Dague, Etienne, Véronique Pons, Alexandre Roland, Jean-Marc Azaïs, Silvia Arcucci, Véronique Lachaize, Samuel Velmont, et al. 2022. "Atomic Force Microscopy-Single-Molecule Force Spectroscopy Unveils GPCR Cell Surface Architecture." *Communications Biology* 5 (1): 221. https://doi.org/10.1038/s42003-022-03162-w.

Davis, Allan Peter, Thomas C Wiegers, Daniela Sciaky, Fern Barkalow, Melissa Strong, Brent Wyatt, Jolene Wiegers, Roy McMorran, Sakib Abrar, and Carolyn J Mattingly. 2025. "Comparative Toxicogenomics Database's 20th Anniversary: Update 2025." *Nucleic Acids Research* 53 (D1): D1328–34. https://doi.org/10.1093/nar/gkae883.

Davis, Sean, and Paul S. Meltzer. 2007. "GEOquery: A Bridge between the Gene Expression Omnibus (GEO) and BioConductor." *Bioinformatics* 23 (14): 1846–47. https://doi.org/10.1093/bioinformatics/btm254.

Dubey, Tushar, and Subashchandrabose Chinnathambi. 2019. “Brahmi (Bacopa Monnieri): An Ayurvedic Herb against the Alzheimer’s Disease.” *Archives of Biochemistry and Biophysics* 676 (November): 108153. https://doi.org/10.1016/j.abb.2019.108153.

Dubey, Tushar, Preeti Kushwaha, H.V. Thulasiram, Madhura Chandrashekar, and Subashchandrabose Chinnathambi. 2023. “Bacopa Monnieri Reduces Tau Aggregation and Tau-Mediated Toxicity in Cells.” *International Journal of Biological Macromolecules* 234 (April): 123171. https://doi.org/10.1016/j.ijbiomac.2023.123171.

Eteleeb, Abdallah M., Brenna C. Novotny, Carolina Soriano Tarraga, Christopher Sohn, Eliza Dhungel, Logan Brase, Aasritha Nallapu, et al. 2024. “Brain High-Throughput Multi-Omics Data Reveal Molecular Heterogeneity in Alzheimer’s Disease.” Edited by Yejin Kim. *PLOS Biology* 22 (4): e3002607. https://doi.org/10.1371/journal.pbio.3002607.

Fatima, Urooj, Sonam Roy, Shahnawaz Ahmad, Lamya Ahmed Al-Keridis, Nawaf Alshammari, Mohd Adnan, Asimul Islam, and Md. Imtaiyaz Hassan. 2022. “Investigating Neuroprotective Roles of Bacopa Monnieri Extracts: Mechanistic Insights and Therapeutic Implications.” *Biomedicine & Pharmacotherapy* 153 (September): 113469. https://doi.org/10.1016/j.biopha.2022.113469.

Fu, Kangyue, Nan Lin, Yiwen Xu, En Huang, Raoli He, Zhixin Wu, Dianbo Qu, Xiaochun Chen, and Tianwen Huang. 2025. “CDK5-Mediated Hyperphosphorylation of Tau217 Impairs Neuronal Synaptic Structure and Exacerbates Cognitive Impairment in Alzheimer’s Disease.” *Translational Psychiatry* 15 (1): 302. https://doi.org/10.1038/s41398-025-03551-9.

Furcila, Diana, Javier DeFelipe, and Lidia Alonso-Nanclares. 2018. “A Study of Amyloid-β and Phosphotau in Plaques and Neurons in the Hippocampus of Alzheimer’s Disease Patients.” *Journal of Alzheimer’s Disease* 64 (2): 417–35. https://doi.org/10.3233/JAD-180173.

Gao, Qi, Yuqiang Fang, Shiqing Zhang, Hung-Wing Li, Ken K. L. Yung, and King Wai Chiu Lai. 2018. “Biophysical Characteristics of Human Neuroblastoma Cell in Oligomeric β -Amyloid (1–40) Cytotoxicity.” *IEEE Transactions on NanoBioscience* 17 (1): 70–77. https://doi.org/10.1109/TNB.2018.2800723.

Grundke-Iqbal, I, K Iqbal, Y C Tung, M Quinlan, H M Wisniewski, and L I Binder. 1986. “Abnormal Phosphorylation of the Microtubule-Associated Protein Tau (Tau) in Alzheimer Cytoskeletal Pathology.” *Proceedings of the National Academy of Sciences* 83 (13): 4913–17. https://doi.org/10.1073/pnas.83.13.4913.

Guler, Ece, Aysen Kopuz, Busra Ertas, Ayse Mine Yilmaz-Goler, Yusufhan Yazir, Deepak M. Kalaskar, and Muhammet Emin Cam. 2024. “Anti-Alzheimer’s Effect of Memantine/Donepezil/Metformin-Loaded PVA/PEO Composite Nanofibers Produced by Pressurized Gyration: Production, Characterization, and in Vitro Evaluation.” *Journal of Drug Delivery Science and Technology* 97 (August): 105795. https://doi.org/10.1016/j.jddst.2024.105795.

Guo, Angyang, Han Wang, Yan Zhang, and Hongbin Huang. 2025. “Changes of the Primary Cilia in Alzheimer’s

Disease Pathogenesis." *European Journal of Neuroscience* 61 (9). https://doi.org/10.1111/ejn.70125.

Hernández-Hernández, Elena, Vladislav A. Petyuk, Júlia Valor-Blanquer, Fernando Yáñez-Gómez, Alasdair M. Barr, Philip L. De Jager, Er-Yun Chen, et al. 2025. "Contributions of Major Tau Kinase Activation and Phospho-Tau Accumulation to Cortical and Hippocampal Tangle Formation and Cognition in Older Adults." *Neurobiology of Disease* 210 (June): 106924. https://doi.org/10.1016/j.nbd.2025.106924.

Hou, Jiahui, Jonathan L. Hess, Chunling Zhang, Jeroen G. J. van Rooij, Gentry C. Hearn, Chun Chieh Fan, Stephen V. Faraone, et al. 2025. "Meta-Analysis of Transcriptomic Studies of Blood and Six Brain Regions Identifies a Consensus of 15 Cross-Tissue Mechanisms in Alzheimer's Disease and Suggests an Origin of Cross-Study Heterogeneity." *American Journal of Medical Genetics Part B: Neuropsychiatric Genetics* 198 (4). https://doi.org/10.1002/ajmg.b.33019.

Huang, Huiqian, Xiaochen Lin, Zhuoyi Liang, Teng Zhao, Shengwang Du, Michael M. T. Loy, Kwok-On Lai, Amy K. Y. Fu, and Nancy Y. Ip. 2017. "Cdk5-Dependent Phosphorylation of Liprinα1 Mediates Neuronal Activity-Dependent Synapse Development." *Proceedings of the National Academy of Sciences* 114 (33). https://doi.org/10.1073/pnas.1708240114.

Islam, Tohidul, Emily Hill, Eric E. Abrahamson, Stijn Servaes, Denis S. Smirnov, Xuemei Zeng, Anuradha Sehrawat, et al. 2025. "Phospho-Tau Serine-262 and Serine-356 as Biomarkers of Pre-Tangle Soluble Tau Assemblies in Alzheimer's Disease." *Nature Medicine* 31 (2): 574–88. https://doi.org/10.1038/s41591-024-03400-0.

Jassal, Bijay, Lisa Matthews, Guilherme Viteri, Chuqiao Gong, Pascual Lorente, Antonio Fabregat, Konstantinos Sidiropoulos, et al. 2019. "The Reactome Pathway Knowledgebase." *Nucleic Acids Research*, November. https://doi.org/10.1093/nar/gkz1031.

Kadhim, Hussam Jawad, Haider Al-Mumen, H. H. Nahi, and S. M. Hamidi. 2022. "Streptozotocin-Induced Alzheimer's Disease Investigation by One-Dimensional Plasmonic Grating Chip." *Scientific Reports* 12 (1): 21878. https://doi.org/10.1038/s41598-022-26607-y.

Kamat, PradipKumar. 2015. "Streptozotocin Induced Alzheimer′s Disease like Changes and the Underlying Neural Degeneration and Regeneration Mechanism." *Neural Regeneration Research* 10 (7): 1050. https://doi.org/10.4103/1673-5374.160076.

Kanehisa, Minoru, Miho Furumichi, Yoko Sato, Mari Ishiguro-Watanabe, and Mao Tanabe. 2021. "KEGG: Integrating Viruses and Cellular Organisms." *Nucleic Acids Research* 49 (D1): D545–51. https://doi.org/10.1093/nar/gkaa970.

Kesavapany, Sashi, Bing-Sheng Li, Niranjana Amin, Ya-Li Zheng, Philip Grant, and Harish C. Pant. 2004. "Neuronal Cyclin-Dependent Kinase 5: Role in Nervous System Function and Its Specific Inhibition by the Cdk5 Inhibitory Peptide." *Biochimica et Biophysica Acta (BBA) - Proteins and Proteomics* 1697 (1–2): 143–53. https://doi.org/10.1016/j.bbapap.2003.11.020.

733 Kevenaar, Josta T., and Casper C. Hoogenraad. 2015. “The Axonal Cytoskeleton: From Organization to Function.”
734 *Frontiers in Molecular Neuroscience* 8 (August). https://doi.org/10.3389/fnmol.2015.00044.

735 Kimura, Taeko, Koichi Ishiguro, and Shin-ichi Hisanaga. 2014. “Physiological and Pathological Phosphorylation of
736 Tau by Cdk5.” *Frontiers in Molecular Neuroscience* 7 (July). https://doi.org/10.3389/fnmol.2014.00065.

737 Kobayashi, Yuki, Shogo Kohbuchi, Noriko Koganezawa, Yuko Sekino, Tomoaki Shirao, Takaomi C. Saido, Takashi
738 Saito, and Yumiko Saito. 2022. “Impairment of Ciliary Dynamics in an APP Knock-in Mouse Model of
739 Alzheimer’s Disease.” *Biochemical and Biophysical Research Communications* 610 (June): 85–91.
740 https://doi.org/10.1016/j.bbrc.2022.04.050.

741 Kruger, Terra M., Kendra J. Bell, Thiranjeewa I. Lansakara, Alexei V. Tivanski, Jonathan A. Doorn, and Lewis L.
742 Stevens. 2019. “Reduced Extracellular Matrix Stiffness Prompts SH-SY5Y Cell Softening and Actin Turnover
743 To Selectively Increase Aβ (1–42) Endocytosis.” *ACS Chemical Neuroscience* 10 (3): 1284–93.
744 https://doi.org/10.1021/acschemneuro.8b00366.

745 Kumari, Raniki, Roshan Kumar, Sanjay Kumar, Abhishek Kumar Singh, Pranita Hanpude, Deepak Jangir, and Tushar
746 Kanti Maiti. 2020. “Amyloid Aggregates of the Deubiquitinase OTUB1 Are Neurotoxic, Suggesting That They
747 Contribute to the Development of Parkinson’s Disease.” *Journal of Biological Chemistry* 295 (11): 3466–84.
748 https://doi.org/10.1074/jbc.RA119.009546.

749 Legleiter, Justin, and Tomasz Kowalewski. n.d. “Atomic Force Microscopy of β-Amyloid: Static and Dynamic Studies
750 of Nanostructure and Its Formation.” In *Atomic Force Microscopy*, 349–64. New Jersey: Humana Press.
751 https://doi.org/10.1385/1-59259-647-9:349.

752 Li, Bin, Muhammad Omar Chohan, Inge Grundke-Iqbal, and Khalid Iqbal. 2007. “Disruption of Microtubule Network
753 by Alzheimer Abnormally Hyperphosphorylated Tau.” *Acta Neuropathologica* 113 (5): 501–11.
754 https://doi.org/10.1007/s00401-007-0207-8.

755 Li, Bing-Sheng, Lei Zhang, Jianguo Gu, Niranjana D. Amin, and Harish C. Pant. 2000. “Integrin α 1 β 1 -Mediated
756 Activation of Cyclin-Dependent Kinase 5 Activity Is Involved in Neurite Outgrowth and Human Neurofilament
757 Protein H Lys-Ser-Pro Tail Domain Phosphorylation.” *The Journal of Neuroscience* 20 (16): 6055–62.
758 https://doi.org/10.1523/JNEUROSCI.20-16-06055.2000.

759 Li, Tong, and Hemant K. Paudel. 2006. “Glycogen Synthase Kinase 3β Phosphorylates Alzheimer’s Disease-Specific
760 Ser 396 of Microtubule-Associated Protein Tau by a Sequential Mechanism.” *Biochemistry* 45 (10): 3125–33.
761 https://doi.org/10.1021/bi051634r.

762 Ma, Guojun, Tong Li, Donald L. Price, and Philip C. Wong. 2005. “APH-1a Is the Principal Mammalian APH-1
763 Isoform Present in γ-Secretase Complexes during Embryonic Development.” *The Journal of Neuroscience* 25
764 (1): 192–98. https://doi.org/10.1523/JNEUROSCI.3814-04.2005.

765 Martens, Marvin, Ammar Ammar, Anders Riutta, Andra Waagmeester, Denise N Slenter, Kristina Hanspers, Ryan A.

Miller, et al. 2021. “WikiPathways: Connecting Communities.” *Nucleic Acids Research* 49 (D1): D613–21. https://doi.org/10.1093/nar/gkaa1024.

Mehla, Jogender, Pooja Gupta, Monika Pahuja, Deepti Diwan, and Diksha Diksha. 2020. “Indian Medicinal Herbs and Formulations for Alzheimer’s Disease, from Traditional Knowledge to Scientific Assessment.” *Brain Sciences* 10 (12): 964. https://doi.org/10.3390/brainsci10120964.

Miller, Emiko, Peter Bambakidis, Niklas Reitsch, Phoebe Templin, Edwin Vázquez-Rosa, Zea Bud, Youngmin Yu, et al. 2024. “Deterioration of Neuronal Primary Cilia in Alzheimer’s Disease.” *Alzheimer’s & Dementia* 20 (S1). https://doi.org/10.1002/alz.093226.

Miller, Nimrod, Zhihua Feng, Brittany M. Edens, Ben Yang, Han Shi, Christie C. Sze, Benjamin Taige Hong, et al. 2015. “Non-Aggregating Tau Phosphorylation by Cyclin-Dependent Kinase 5 Contributes to Motor Neuron Degeneration in Spinal Muscular Atrophy.” *The Journal of Neuroscience* 35 (15): 6038–50. https://doi.org/10.1523/JNEUROSCI.3716-14.2015.

Mokhtar, Sara H., Maha M. Bakhuraysah, David S. Cram, and Steven Petratos. 2013. “The Beta-Amyloid Protein of Alzheimer’s Disease: Communication Breakdown by Modifying the Neuronal Cytoskeleton.” *International Journal of Alzheimer’s Disease* 2013: 1–15. https://doi.org/10.1155/2013/910502.

Narayanan, Manikandan, Jimmy L Huynh, Kai Wang, Xia Yang, Seungyeul Yoo, Joshua McElwee, Bin Zhang, et al. 2014. “Common Dysregulation Network in the Human Prefrontal Cortex Underlies Two Neurodegenerative Diseases.” *Molecular Systems Biology* 10 (7): MSB145304. https://doi.org/10.15252/msb.20145304.

Nascimento Amorim, Maria do Socorro do, Álefe Roger Silva França, Ralph Santos-Oliveira, Jonas Rodrigues Sanches, Thamys Marinho Melo, Bruno Araújo Serra Pinto, Leandro R. S. Barbosa, and Luciana Magalhães Rebelo Alencar. 2024. “Atomic Force Microscopy Applied to the Study of Tauopathies.” *ACS Chemical Neuroscience* 15 (4): 699–715. https://doi.org/10.1021/acschemneuro.3c00819.

Neddens, Joerg, Magdalena Temmel, Stefanie Flunkert, Bianca Kerschbaumer, Christina Hoeller, Tina Loeffler, Vera Niederkofler, Guenther Daum, Johannes Attems, and Birgit Hutter-Paier. 2018. “Phosphorylation of Different Tau Sites during Progression of Alzheimer’s Disease.” *Acta Neuropathologica Communications* 6 (1): 52. https://doi.org/10.1186/s40478-018-0557-6.

Nishida, Kohei, Kosuke Matsumura, Miki Tamura, Takuto Nakamichi, Keiya Shimamori, Masahiro Kuragano, Arif Md. Rashedul Kabir, et al. 2023. “Effects of Three Microtubule-Associated Proteins (MAP2, MAP4, and Tau) on Microtubules’ Physical Properties and Neurite Morphology.” *Scientific Reports* 13 (1): 8870. https://doi.org/10.1038/s41598-023-36073-9.

Pardossi-Piquard, Raphaëlle, Seung-Pil Yang, Soshi Kanemoto, Yongjun Gu, Fusheng Chen, Christopher Böhm, Jean Sevalle, et al. 2009. “APH1 Polar Transmembrane Residues Regulate the Assembly and Activity of Presenilin Complexes.” *Journal of Biological Chemistry* 284 (24): 16298–307. https://doi.org/10.1074/jbc.M109.000067.

Paszternák, Alexandra, Kamilla Varga, Ramá Gyöngyössy, Katinka Tarnóczi, Noémi Sikur, Éva Szökő, and Tamás Tábi. 2025. "Resveratrol Analogs Ameliorate Mitochondrial Impairment and Insulin Resistance in a Streptozotocin-Induced In Vitro Model of Alzheimer's Disease." *International Journal of Molecular Sciences* 26 (21): 10787. https://doi.org/10.3390/ijms262110787.

Phrompittayarat, W., Putalun, W., Tanaka, H., Jetiyanon, K., Wittaya-areekul, S., Ingkaninan, K. 2007. "Comparison of Various Extraction Methods of Bacopa Monnieri." *Asian Health, Science and Technology Reports* 15(1): 29–34. https://ph03.tci-thaijo.org/index.php/ahstr/article/view/2433.

Plaschke, Konstanze, and Jürgen Kopitz. 2015. "In Vitro Streptozotocin Model for Modeling Alzheimer-like Changes: Effect on Amyloid Precursor Protein Secretases and Glycogen Synthase Kinase-3." *Journal of Neural Transmission* 122 (4): 551–57. https://doi.org/10.1007/s00702-014-1319-7.

Regalado-Reyes, Mamen, Diana Furcila, Félix Hernández, Jesús Ávila, Javier DeFelipe, and Gonzalo León-Espinosa. 2019. "Phospho-Tau Changes in the Human CA1 During Alzheimer's Disease Progression." *Journal of Alzheimer's Disease* 69 (1): 277–88. https://doi.org/10.3233/JAD-181263.

Ritchie, Matthew E., Belinda Phipson, Di Wu, Yifang Hu, Charity W. Law, Wei Shi, and Gordon K. Smyth. 2015. "Limma Powers Differential Expression Analyses for RNA-Sequencing and Microarray Studies." *Nucleic Acids Research* 43 (7): e47–e47. https://doi.org/10.1093/nar/gkv007.

Safran, Marilyn, Naomi Rosen, Michal Twik, Ruth BarShir, Tsippi Iny Stein, Dvir Dahary, Simon Fishilevich, and Doron Lancet. 2021. "The GeneCards Suite." In *Practical Guide to Life Science Databases*, 27–56. Singapore: Springer Nature Singapore. https://doi.org/10.1007/978-981-16-5812-9_2.

Sahu, Manas Ranjan, Mir Hilal Ahmad, and Amal Chandra Mondal. 2026. "Xmu-Mp-1 Attenuates Streptozotocin-Induced Neurotoxicity in SH-SY5Y Cells: Potential Role of Hippo Pathway Modulation." *Molecular Biology Reports* 53 (1): 384. https://doi.org/10.1007/s11033-026-11561-z.

Shalini, Vijayanna Tirumalapura, Sajjanar Jambappa Neelakanta, and Jaideep Sitaram Sriranjini. 2021. "Neuroprotection with Bacopa Monnieri–A Review of Experimental Evidence." *Molecular Biology Reports* 48 (3): 2653–68. https://doi.org/10.1007/s11033-021-06236-w.

Shandilya, Shruti, Kavindra Kumar Kesari, and Janne Ruokolainen. 2021. "Vitamin K2 Modulates Organelle Damage and Tauopathy Induced by Streptozotocin and Menadione in SH-SY5Y Cells." *Antioxidants* 10 (6): 983. https://doi.org/10.3390/antiox10060983.

Shannon, Paul, Andrew Markiel, Owen Ozier, Nitin S. Baliga, Jonathan T. Wang, Daniel Ramage, Nada Amin, Benno Schwikowski, and Trey Ideker. 2003. "Cytoscape: A Software Environment for Integrated Models of Biomolecular Interaction Networks." *Genome Research* 13 (11): 2498–2504. https://doi.org/10.1101/gr.1239303.

Shin, Saewoon, Xiaohui Zhu, Sarnai Amartumur, Taehoon Lee, Won Jong Yu, Soomin Park, Niloofar Etemadi, et al.

2026. “Human Brain and Organoid Transcriptomes Reveal Key Receptor Tyrosine Kinase Pathways and Genetic Signatures in Alzheimer’s Disease.” *Experimental & Molecular Medicine* 58 (4): 1230–41. https://doi.org/10.1038/s12276-026-01684-5.

Singh, Abhishek, Shubhangini Tiwari, and Sarika Singh. 2024. “Pirh2 Modulates the Mitochondrial Function and Cytochrome C-Mediated Neuronal Death during Alzheimer’s Disease.” *Cell Death & Disease* 15 (5): 331. https://doi.org/10.1038/s41419-024-06662-1.

Smyth, Gordon K. 2004. “Linear Models and Empirical Bayes Methods for Assessing Differential Expression in Microarray Experiments.” *Statistical Applications in Genetics and Molecular Biology* 3 (1): 1–25. https://doi.org/10.2202/1544-6115.1027.

Stephens, Morgan C., Jiayang Li, Megan Mair, Justin Moore, Katy Zhu, Akash Tarkunde, Bismark Amoh, et al. 2025. “Computational and Functional Prioritization Identifies Genes That Rescue Behavior and Reduce Tau Protein in Fly and Human Cell Models of Alzheimer Disease.” *The American Journal of Human Genetics* 112 (5): 1081–96. https://doi.org/10.1016/j.ajhg.2025.03.012.

Sumathi, Thangarajan, Mohamed Nayeem, Kedike Balakrishna, Gopalsamy Veluchamy, and Sivasithamparam Niranjali Devaraj. 2002. “Alcoholic Extract of ‘Bacopa Monniera’ Reduces the in Vitro Effects of Morphine Withdrawal in Guinea-Pig Ileum.” *Journal of Ethnopharmacology* 82 (2–3): 75–81. https://doi.org/10.1016/S0378-8741(02)00139-3.

Sushma, Manas Ranjan Sahu, Natarajan Arul Murugan, and Amal Chandra Mondal. 2024. “Amelioration of Amyloid-β Induced Alzheimer’s Disease by Bacopa Monnieri through Modulation of Mitochondrial Dysfunction and GSK-3β/Wnt/β-Catenin Signaling.” *Molecular Nutrition & Food Research* 68 (13). https://doi.org/10.1002/mnfr.202300245.

Szklarczyk, Damian, Rebecca Kirsch, Mikaela Koutrouli, Katerina Nastou, Farrokh Mehryary, Radja Hachilif, Annika L Gable, et al. 2023. “The STRING Database in 2023: Protein–Protein Association Networks and Functional Enrichment Analyses for Any Sequenced Genome of Interest.” *Nucleic Acids Research* 51 (D1): D638–46. https://doi.org/10.1093/nar/gkac1000.

Tanaka, Teruyuki, Veeranna, Toshio Ohshima, Prithi Rajan, Niranjana D. Amin, Andrew Cho, Taduru Sreenath, Harish C. Pant, Roscoe O. Brady, and Ashok B. Kulkarni. 2001. “Neuronal Cyclin-Dependent Kinase 5 Activity Is Critical for Survival.” *The Journal of Neuroscience* 21 (2): 550–58. https://doi.org/10.1523/JNEUROSCI.21-02-00550.2001.

Thal, Dietmar R., Udo Rüb, Mario Orantes, and Heiko Braak. 2002. “Phases of Aβ-Deposition in the Human Brain and Its Relevance for the Development of AD.” *Neurology* 58 (12): 1791–1800. https://doi.org/10.1212/WNL.58.12.1791.

Tiraboschi, P., L. A. Hansen, L. J. Thal, and J. Corey-Bloom. 2004. “The Importance of Neuritic Plaques and Tangles

to the Development and Evolution of AD." *Neurology* 62 (11): 1984–89. https://doi.org/10.1212/01.WNL.0000129697.01779.0A.

Todd, Nicholas K., Yunhong Huang, Ji Young Lee, Pemra Doruker, James M. Krieger, Ryan Salisbury, Matthew MacDonald, Ivet Bahar, and Amantha Thathiah. 2022. "GPCR Kinases Generate an APH-1A Phosphorylation Barcode to Regulate Amyloid-β Generation." *Cell Reports* 40 (3): 111110. https://doi.org/10.1016/j.celrep.2022.111110.

Vinod, Adithya, Sankaran Sathianarayanan, Anju Elizabath Babu, Prashant Sadanandan, Athira Kaipuzha Venu, and Baskar Venkidasamy. 2022. "Bacopa Monnieri for Disorders Affecting Brain: Current Perspectives." *Current Topics in Medicinal Chemistry* 22 (23): 1909–29. https://doi.org/10.2174/1568026622666220119111538.

Vossel, Keith A., Jordan C. Xu, Vira Fomenko, Takashi Miyamoto, Elsa Suberbielle, Joseph A. Knox, Kaitlyn Ho, Daniel H. Kim, Gui-Qiu Yu, and Lennart Mucke. 2015. "Tau Reduction Prevents Aβ-Induced Axonal Transport Deficits by Blocking Activation of GSK3β." *Journal of Cell Biology* 209 (3): 419–33. https://doi.org/10.1083/jcb.201407065.

Vossel, Keith A., Kai Zhang, Jens Brodbeck, Aaron C. Daub, Punita Sharma, Steven Finkbeiner, Bianxiao Cui, and Lennart Mucke. 2010. "Tau Reduction Prevents Aβ-Induced Defects in Axonal Transport." *Science* 330 (6001): 198–198. https://doi.org/10.1126/science.1194653.

Wan, Ying-Wooi, Rami Al-Ouran, Carl G. Mangleburg, Thanneer M. Perumal, Tom V. Lee, Katherine Allison, Vivek Swarup, et al. 2020. "Meta-Analysis of the Alzheimer's Disease Human Brain Transcriptome and Functional Dissection in Mouse Models." *Cell Reports* 32 (2): 107908. https://doi.org/10.1016/j.celrep.2020.107908.

Yeo, Seungeun, Jaemyung Jang, Hyun Jin Jung, Hyeyoung Lee, and Youngshik Choe. 2023. "Primary Cilia-Mediated Regulation of Microglial Secretion in Alzheimer's Disease." *Frontiers in Molecular Biosciences* 10 (October). https://doi.org/10.3389/fmolb.2023.1250335.

Yu, Yang, Xiaoqin Run, Zhihou Liang, Yi Li, Fei Liu, Ying Liu, Khalid Iqbal, Inge Grundke-Iqbal, and Cheng-Xin Gong. 2009. "Developmental Regulation of Tau Phosphorylation, Tau Kinases, and Tau Phosphatases." *Journal of Neurochemistry* 108 (6): 1480–94. https://doi.org/10.1111/j.1471-4159.2009.05882.x.

Zheng, Ya-Li, Sashi Kesavapany, Maneth Gravell, Rebecca S Hamilton, Manfred Schubert, Niranjana Amin, Wayne Albers, Philip Grant, and Harish C Pant. 2005. "A Cdk5 Inhibitory Peptide Reduces Tau Hyperphosphorylation and Apoptosis in Neurons." *The EMBO Journal* 24 (1): 209–20. https://doi.org/10.1038/sj.emboj.7600441.

Acknowledgements

We are very grateful to Dr. Pradeep Punnakkal, Department of Biophysics, Post Graduate Institute of Medical Education and Research (PGIMER), Chandigarh, India, for his scientific valuable insight and suggestions for our manuscript. We would like to thank Advanced Instrumentation Research Facility (AIRF) and Common Instrumentation Facility (CIF), School of Biotechnology (SBT), Jawaharlal Nehru University, New Delhi, India. We

are very thankful to the Faculty of Life Sciences and Biotechnology (FLSB), South Asian University (SAU) for confocal imaging facility. We would also like to thank all the members of Laboratory of Optobiotechnology, SBT, JNU and Aman Murari (Ph.D. Scholar) from PGIMER, Chandigarh, India.

Funding

Authors would like to thank Indian Institute of Medical Research (ICMR), New Delhi, India for providing research grant (2021-13707) fund to carry out part of this research work. Umesh Prasad Sah Hathi would also like to thank ICMR for appointment for the position of Research Scientist-I under the above mentioned project.

Contributions

Umesh Prasad Sah Hathi: Writing-original draft, review & edit, Visualization, Investigation, Formal analysis and Data curation (system biology, cell culture, transcriptomics and imaging). Abhishek Kumar: Writing-review & edit, Investigation (computational biology), Formal analysis, Data Curation. Jyotsna Arora: Writing-review & edit, Investigation (Phytochemicals extraction, and computational biology), Formal analysis, Data Curation (LC-MS/GC-MS analysis). Suneel Kateriya: Writing-review & editing, Supervision, Funding acquisition, Conceptualization.

Ethics declarations

Conflict of interest

The authors declare that they do not have any financial interests or personal relationships that could influence the work reported in this paper.

Supplementary Files

This is a list of supplementary files associated with this preprint. Click to download.

- SupplementaryInformationSI.docx